Proceedings of the Iowa Academy of Science

Volume 75 | Annual Issue Article 37

1968

Rocket and Satellite Studies of the X-Ray Emission from the Quiescent Sun

P. R. Sengupta
University of Iowa

Rocket and Satellite Studies of the X-Ray Emission from the Quiescent Sun[1]

P. R. SENGUPTA[2]

Abstract. Quiescent sun x-ray measurements made by different workers during the past 19 years have been studied. Analysis of the data available up to April, 1967, confirms the conclusion that the quiescent sun x-ray emission is thermal in nature and is closely related to the solar activity level. The spectrum below 18 Å is mainly continuous and is primarily due to recombination emission. Bremsstrahlung becomes important at high temperatures. The 18 — 100 Å flux is primarily due to line emission and is emitted mainly by the undisturbed coronal regions. Below 20 Å the emission is primarily from the active — hotter and denser — coronal regions. In this spectral region the flux varies within wide limits, depending on the number, dimensions, density and temperature of the active regions. Preferred regions of x-ray emission lie above strong calcium plages in the chromosphere and coincide with regions of enhanced centimeter radio emission. Seventy-five percent of the total x-ray flux comes from these regions. The existing theory is capable of predicting x-ray flux within a factor of 2 or 3, using solar radio spectro-heliograms in the centimeter range.

The study of the x-ray emission of the sun is an important part of space science research. It is now known that solar x rays are generated in the solar corona and carry important information about the composition, structure, and state of the corona, and about the physical processes which occur in it. Study of this radiation is, therefore, of great importance in solar physics. Moreover, this radiation is partly responsible for the formation of the ionosphere and is presumably primarily responsible for the S.I.D.s (Sudden Ionospheric Disturbances); as such it forms an important part of solar terrestial relations. Solar x-ray study is also vey important to space material technology for the effect the x rays produce on the surface properties of the materials used in rockets and satellites. Hence, it is important to know the intensity of x rays outside the earth's atmosphere.

Electromagnetic radiation of wavelength shorter than 2900 Å is wholly absorbed by the earth's atmosphere above 40 km altitude and can be directly investigated only with the help of high altitude rockets and artificial earth satellites. The first experimental study of solar x rays was made by Burnight (1949) and Tousey et al. (1951) with the aid of V2 rockets. Friedman et al. began their experimental studies in 1949. The first theoretical calculation of the solar x-ray flux was performed by Sklovskij (1949). This was followed by many experiments and calculations carried out by different group of workers in various countries.

[1]This work was supported in part by the National Aeronautics and Space Administration under Contract No. NAS5-9076.

[2]Department of Physics and Astronomy, The University of Iowa, Iowa City, Iowa.

The x-ray spectrum of the quiescent sun extends from a few angstroms in the shortwave side to ultraviolet radiation in the longwave side. Emission from the disturbed sun extends up to photons of energy greater than 200 keV during strong flares. The upper energy limit of the solar flare photon is not yet fully established. X-ray emission from the quiescent sun will be considered in the present paper.

Experimental Study

X-Ray Detectors. X-ray flux is measured by photon counters or ionization chambers with windows made of thin filtering films of beryllium, mica, aluminum, or organic materials like mylar. Measurements are made largely in the spectral regions 2 — 8 Å, 8 — 20 Å, and 44 — 60 Å. The choice of these wavelength ranges is imposed by instrumental considerations like the filtering properties of the thin window films used and the efficiency of the counters in the different wavelength regions.

Table 1 gives a description of the detectors used in Naval Research Laboratory rockets. 2 — 20 keV and 20 — 200 keV detectors were used for flare x-ray measurement. Figure 1 shows the typical spectral sensitivity range of the 8 — 10 Å detector while Figure 2 shows the spectral sensitivity of the 2 — 8 Å detector used in N.R.L. rocket experiments.

Table 1

Description of the Detectors Used in N.R.L. Rocket Experiments

Spectral Region	Type of Detector	Window	Gas or Crystal	Type of Output
2-20 keV	Proportional counter	Beryllium 24.4 mg/cm^2	Ne + CO_2	Pulses Amplitude Preserved
20-200 keV	Scintillation counter	Beryllium 156 mg/cm^2 + Aluminum	Na I	— Do —
2-8 Å	Geiger counter	Beryllium 24.4 mg/cm^2	Ne + Ethyl Formate	Counting rate meter
8-20 Å	— Do —	Aluminum 1.534 mg/cm^2	— Do —	— Do —
44-60 Å	Ion Chamber	Mylar .841 mg/cm^2	Nitrogen	Current

As the spectral bandwidth of the detector is broad, it is necessary to assume a spectral energy distribution for converting the detector signal to the energy recorded in a given spectral region. N.R.L. group of workers assumed that the energy distribution in the solar spectrum is that of a grey body, i.e.,

$$I(\nu) = \frac{c}{\nu 3} \times \frac{1}{e^{h\nu/kT_g} - 1} .$$

Three different values of T_g have to be used for interpreting data in

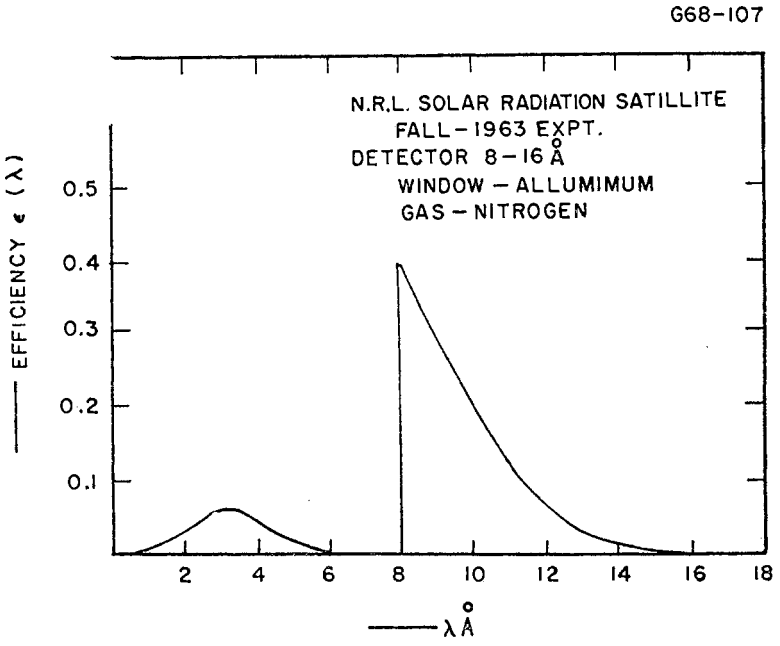

Figure 1. N.R.L. Solar radiation satellite, Fall-1963 experiment, 8-16 Å detector efficiency. (After Kreplin.)

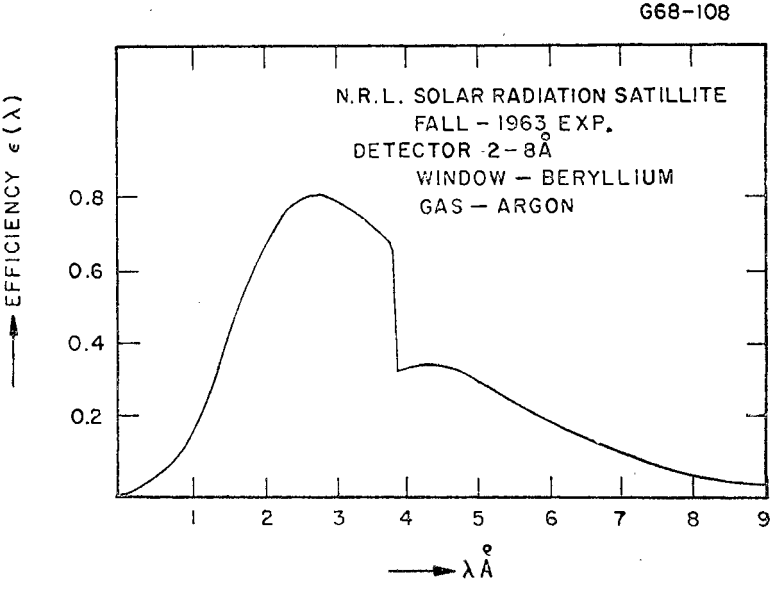

Figure 2. N.R.L. Solar radiation satellite, Fall-1963 experiment, 2-8 Å detector efficiency. (After Kreplin.)

Table 2

X-Ray Flux from the Quiet Sun Recorded in Rocket Experiments Extrapolated to the Boundary of the Earth's Atmosphere

Expt. No.	Date	Region I Spectral Region Å	Region I Energy erg/cm² sec	Region II Spectral Region Å	Region II Energy erg/cm² sec	Region III Spectral Region Å	Region III Energy erg/cm² sec	Reference and Notes
1	Sept. 29, 1949	2-8	1.5×10^{-3}					Bryam et al. (1956)
								Kreplin (1961); 2½ hrs. following class 1 flare
2	May 1, 1952	2-8	1.7×10^{-3}					" Tg = 2×10^{6}°
3	May 5, 1952	2-8	$< 5 \times 10^{-4}$					" $\Delta\lambda$ = 2-8 & 8-20 Å
4	Nov. 15, 1953	2-8	$< 7 \times 10^{-6}$	8-20	$< 1.5 \times 10^{-3}$	44-100	6.4×10^{-2}	" Tg = 0.5×10^{6}°
5	Nov. 25, 1953	2-8	3×10^{-6}	8-20	1.3×10^{-3}			" $\Delta\lambda$ = 44-100 Å
6	Dec. 1, 1953			8-20	0.39×10^{-3}	44-60	2.3×10^{-2}	"
						44-100	5.3×10^{-2}	"
7	Oct. 18, 1955			8-20	1.5×10^{-3}			
8	Dec. 21, 1959 morning	2-10 (2-8)	7.3×10^{-4} (3.6×10^{-4})					Mandel 'stam et al. (1961a) Te ≈ 4.5×10^{6}°
9	Dec. 21, 1959 evening	2-10 (2-8)	3.2×10^{-4} (1.6×10^{-4})					"
10	Aug. 7, 1959	2-8	1.0×10^{-3}	8-20	2.3×10^{-2}			Chubb et al. (1960); sub-flare
11	Aug. 14, 1959	2-8	1.0×10^{-3}	8-20	2.3×10^{-2}	44-60	8.5×10^{-2}	"
12	Aug. 29, 1959	2-8	3.3×10^{-3}			44-60	1.7×10^{-2}	"
13	Sept. 17, 1959			8-15	1.1×10^{-2}			Pounds & Sanford (1963) Tg = 1.7×10^{6}°
14	Nov. 23, 1960			8-15	2.7×10^{-2}			" Tg = $1.7\text{-}2.1 \times 10^{6}$°
15	Sept. 27, 1961	2-8	1.5×10^{-3}	8-14	2.2×10^{-2}			" Tg = 3×10^{6} for $\Delta\lambda$ = 2-8 Å
16	Oct. 24, 1961			8-15	$1\text{-}1.5 \times 10^{-2}$			" Tg = $1.2\text{-}2 \times 10^{6}$° for $\Delta\lambda$ = 8-14 Å
17	Oct. 18, 1962	2-10	1.7×10^{-4}	8-18	1.4×10^{-2}			Tindo & Surygin (1965)
18	1963-64	< 8	5×10^{-5} —	8-12	2×10^{-4}	44-60	1.3×10^{-2}	Pounds (1965) Minimum flux from 4 flights near activity minimum.

the three spectral bands. These values are $T_g = 0.5 \times 10^6$°K for 44 — 60 Å, $T_g = 1.5 \times 10^6$ to 2×10^6°K for 8 — 20 Å, and $T_g = 2 \times 10^6$ to 2.5×10^6°K for 0 — 8 Å. These assumptions obtain support from the existing theoretical models of solar x-ray emission.

Rocket Experiments. Experiments were carried out in the early fifties with the aid of high altitude rockets. Rocket measurements give the x-ray flux during the short time spent by detectors outside the earth's atmosphere and also give the instantaneous flux corresponding to solar conditions at that time.

Table 2 gives a summary of results of American, British, and Soviet rocket measurements of the quiescent sun x-ray flux during the period 1949 to 1962, i.e., for a period greater than one solar cycle.

From the table it is seen that the quiescent sun x-ray flux extrapolated to the boundary of the earth's atmosphere varied during one solar cycle from minimum to maximum. In detail,

1. $\approx 10^{-6}$ to $\approx 10^{-3}$ erg/cm^2 sec, i.e., by a factor of 1000 in the wavelength range 0 — 10 Å.

2. $\approx 10^{-4}$ to 10^{-2} erg/cm^2 sec, i.e., by a factor of 100 in the wavelength range 10 — 20 Å.

3. 1.3×10^{-2} to 8.5×10^{-2} erg/cm^2 sec, i.e., by a factor of 7 in the wavelength range 44 — 60 Å.

The table shows that there is a good correlation between x-ray flux and the eleven-year cycle of solar activity. According to Friedman, solar flux increased by factors of 600 — 1000, 60 and 7 in the 2 — 8, 8 — 20, and 44 — 60 Å ranges, respectively, between the 1953 minimum and the 1958 maximum. His figures are in agreement with the figures obtained from Table 2.

Satellite Experiments. Satellite measurements are more useful than rocket measurements because they cover extended periods of time and provide information about the dynamic changes in the x-ray intensity, the correlation between variations in the intensity and changes in solar activity, and hence the x-ray flux characteristic for a mean solar activity level over a given time, say a day, a month, or a year. Further, they can record faithfully the complete time profile of a solar disturbance such as a solar flare.

Data available to this date are from American satellites: N.R.L. SR-1, N.R.L. SR-3, Injun I (U. I. experiment), Injun III (U. I. experiment), N.R.L. SR-4 (1964-01D), OSO-I, VELA I, VELA II, OSO-II, OSO-III, N.R.L. 1965-16D, Explorer 30 (N.R.L. SR-8), Explorer 33 (U. I. experiment), Explorer 35 (U. I. experiment), and Mariner V (U. I. experiment); British satellite: Ariel I; and Russian satellites: Spaceship 2, Spaceship 3, Electron 2, and Electron 4.

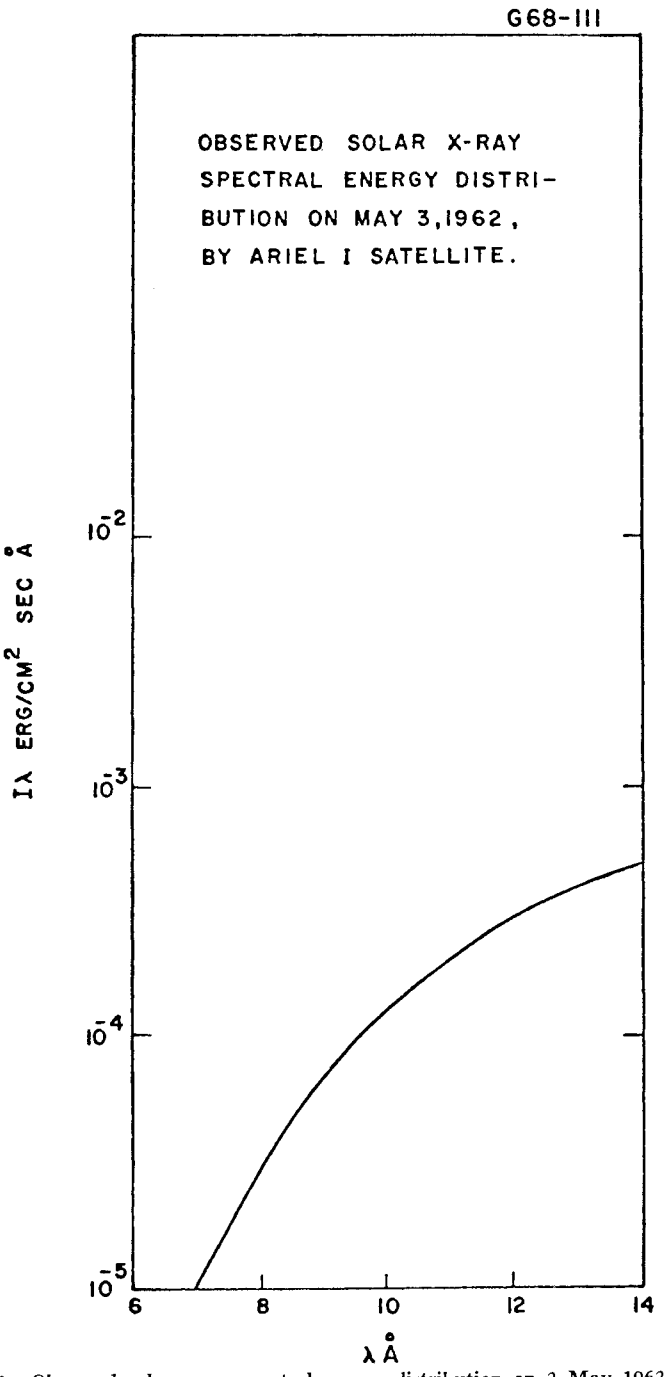

Figure 3. Observed solar x-ray spectral energy distribution on 2 May 1962 measured by Ariel I satellite.

The British satellite Ariel I detector included a spectrum analyzer in 5 — 14 A° band. A typical spectral energy distribution of the quiescent sun obtained from Ariel I is shown in Figure 3. This distribution cannot be represented by a grey body distribution with a single temperature. Different parts of this spectral region correspond to $T_g = 1.8 \times 10^{6}$°K, 1.6×10^{6}°K, 1.45×10^{6}°K, and 1.3×10^{6}°K for 7 — 9, 9 — 11, 11 — 13, and 13 — 15 Å, respectively.

The U. I. detectors on Explorer 33 comprise three EON 6213 mica-windowed geiger counters GM1, GM2, and GM3. Figure 4 shows the arrangement of these detectors on Explorer 33. GM1 has a fan-shaped aperture and its axis is orthogonal to the spin axis. GM2 has a conical aperture of 20° half-angle and its axis is parallel to the spin axis of the satellite. GM3, which is identical to GM2, has its axis antiparallel to the spin axis. The three counters face the sun one after

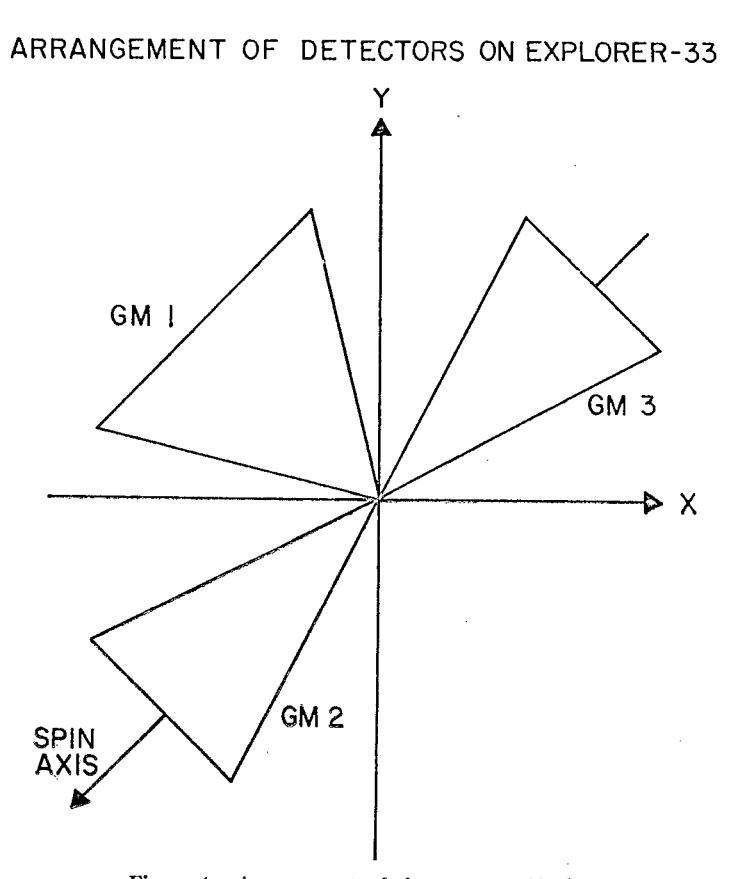

Figure 4. Arrangement of detectors on Explorer 33.

another in the course of a year with a 19-day interval when no counter sees the sun. The angle between the sun and the detector axis varies continuously and can be calculated knowing the position of the satellite. A correction in the signal due to aspect angle is available for each detector. The time resolution of the telemetered signal is 81 seconds and the telemetry is independent of spin period. The counters record charged particles in addition to x rays. The particle flux is subtracted from the total signal to obtain the x-ray flux (Van Allen, 1967).

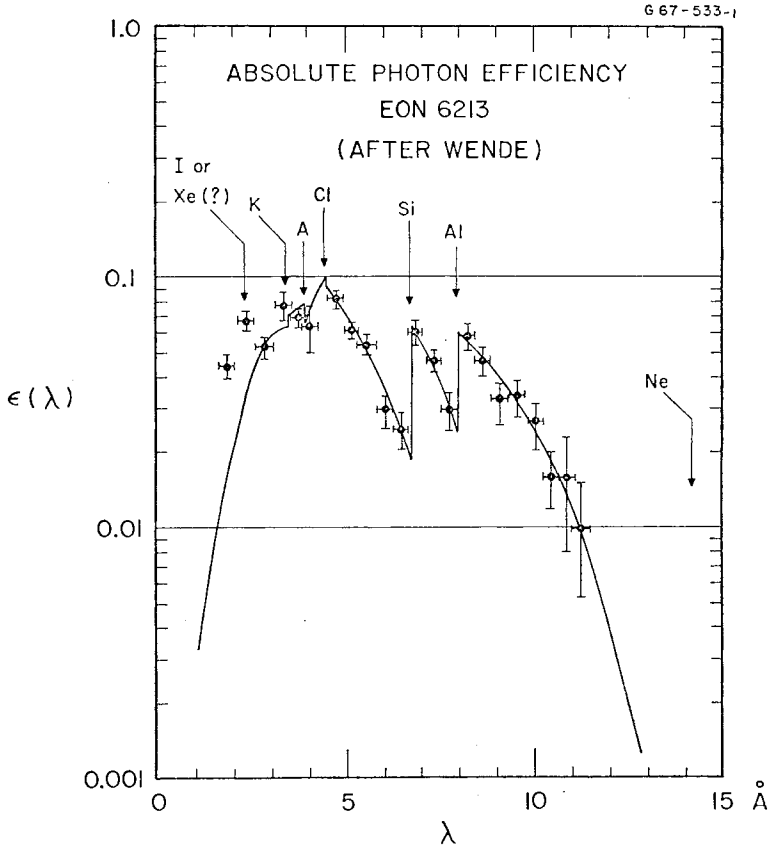

Figure 5. Absolute photo efficiency of Explorer 33 x-ray detector.

Figure 5 shows the photon efficiency of these detectors. Figure 6 shows the 2 — 12 Å flux recorded by the U. I. detector on Explorer 33 on 21 August 1966. This was a quiet day. Figure 7 shows the recorded flux on 3 August 1966. This was a disturbed day.

The following conclusions can be drawn from the satellite measurements during the past nine years: (1) The 20 — 100 Å flux remains

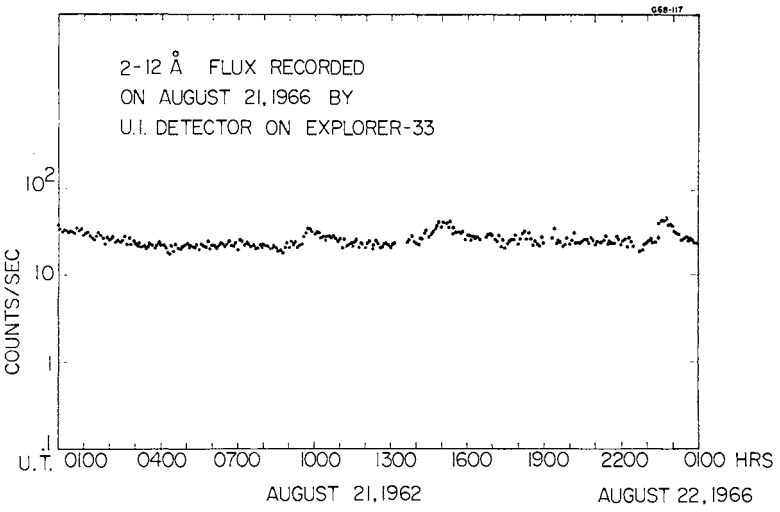

Figure 6. 2-12 Å flux recorded on 21 August 1966 by U.I. detector on Explorer 33.

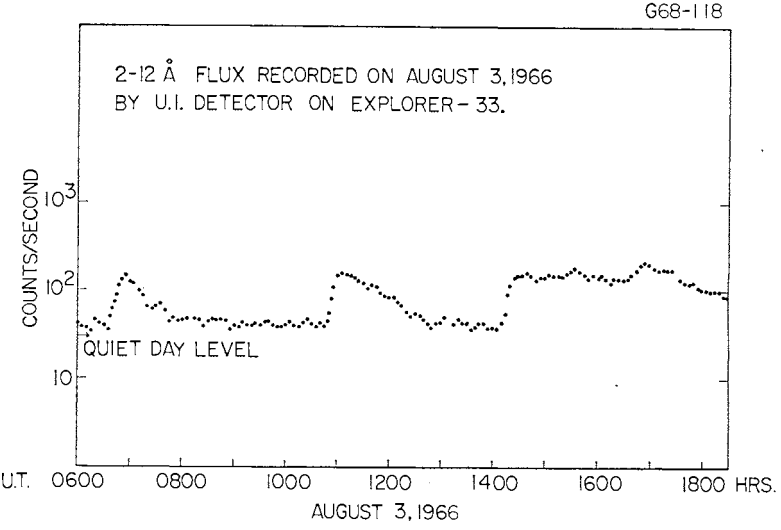

Figure 7. 2-12 Å flux recorded on 3 August 1966 by U.I. detector on Explorer 33.

practically constant over time intervals of the order of 24 hours. (2) The 0 — 10 Å x-ray flux shows variations over periods of less than 24 hours. (3) Over longer periods of time, the intensity below 20 Å is subject to considerable variations. Below 10 Å the intensity may vary by a factor of 20 to 200 over a period of a few weeks, while in the 10 — 20 Å range, it may change by an order of magnitude; the 44 — 60 Å flux is much more steady. It does not change

by a factor of more than 2 — 3. (4) For still longer periods of time, between 1959 and 1964, i.e., the period covering conditions approaching both maximum and minimum solar activity, the intensity of radiation from the quiescent sun lies within the following limits:

$\lambda < 8$ Å $\approx 5 \times 10^{-6}$ to $\approx 10^{-3} - 1.5 \times 10^{-3}$ erg/cm^2 sec
$\lambda < 10$ Å $\approx 10^{-5}$ to $\approx 2 \times 10^{-3} - 5 \times 10^{-3}$ erg/cm^2 sec
10 — 20 Å $\approx 10^{-4}$ to $\approx 10^{-2} - 6 \times 10^{-2}$ erg/cm^2 sec
44 — 60 Å $\approx 5 \times 10^{-2}$ to $\approx 4 \times 10^{-1}$ erg/cm^2 sec.

These data are in agreement with rocket data. (5) Variations in the x-ray intensity of the quiescent sun are closely associated with centimeter wave solar radio emission. The 0 — 20 Å flux is seen to be fairly well correlated with centimeter wave radio emission, but the correlation is not complete; the amplitude of the 0 — 20 Å flux variation is much higher than that of centimeter radio flux variation. (6) The 0 — 20 Å x-ray flux variation is closely associated with relative sunspot numbers. The association is poorer with the 20 — 100 Å flux. A fairly good correlation exists between the E layer index and the 30 — 100 Å solar x-ray flux (Sengupta, 1968).

Theory of X-Ray Emission and Comparison with Experimental Observations

There are three components of the coronal radiation:

(1) Free-free transitions of electrons in the field of positive ions. This phenomenon is also called bremsstrahlung. A thermal bremsstrahlung is due to electrons having thermal (Maxwellian) distribution.

(2) A free-bound component of the continuum due to recombination of electrons with the heavy ions of the coronal plasma.

(3) Line emission particularly in the region 40 — 100 Å. Some of the emission lines are due to de-excitation of an upper level by recombination; the greater part, however, is the result of direct excitation by electron impacts.

The first two components give the continuum radiation.

Assuming that x-ray emission of the quiescent sun is of thermal origin, the intensity of bremsstrahlung emitted per unit volume in a frequency range $d\upsilon$ can be approximately taken to be (Elwert, 1954)

$$I^{ff} d\upsilon = \sum_z \sum_i N_{z,i}\ Ne\ C\ zi^2 \left(\frac{\chi_H}{kTe}\right)^{1/2} \exp\left(\frac{-h\upsilon}{kTe}\right) d\upsilon \qquad (1)$$

where $C = \approx 1.7 \times 10^{-40}$ erg/cm^3, z is the atomic number of the element, $N_{z,i}$ is the number of ions with atomic number z, whose degree of ionization is i, $\chi_{z,i}$ is the ionization potential of this ion

in the ground state, χ_H is the ionization potential of Hydrogen, h is Planck's constant, and K is Boltzman's constant. The double summation extends over all ions of all elements. For the recombination radiation we have

$$I^{fg}\, d\upsilon = \sum_z \sum_i N_{z,i}\, Ne\, C \left(\frac{\chi_H}{kTe}\right)^{3/2} \left(\frac{\chi_{z,i}}{y_H}\right)^2 \times \frac{\zeta_{z,i}}{m_o} \exp\left(\frac{\chi_{z,i} - h\upsilon}{kTe}\right) d\upsilon \qquad (2)$$

where $\zeta_{z,i}$ is the number of electrons in the outer shell of the given ion, m_o is the principal quantum number of the ground state, and y_H is emission measure for Hydrogen. The double summation extends over all ions of all elements whose ionization limit is $\upsilon_{z,i} \leq \upsilon$.

For the line emission corresponding to optical electron transitions, we have

$$I^L = \sum_z \sum_i N_{z,i}\, Ne\, h\upsilon_{z,i} <\sigma\, \upsilon> \qquad (3)$$

where $<\sigma\, \upsilon>$ is the cross-section for the excitation of the upper level of the given line averaged over Maxwellian distribution. This cross-section is given by the approximate formula (Allen, 1963)

$$<\sigma\, \upsilon> = 17 \times 10^{-4} \frac{f}{Te^{1/2}w}\, 10^{-5040w/Te}\, P\left(\frac{w}{kTe}\right) \qquad (4)$$

where f is the oscillator strength of the line, w is the excitation energy in electron volts, and P(w/kTe) is a tabulated correction factor. Comparison with the cross-section calculated on the Born-Coulomb approximation has shown that errors introduced by using Equation (4) are not substantial.

Table 3 shows computed energy distribution between 2 and 20 Å for $T_e = 2 \times 10^6$°K. Table 4 shows computed energy distribution between 20 and 100 Å for $T_e = 1 \times 10^6$°K. Table 5 shows the relative contribution of the various processes to x-ray intensity in 2 — 20 Å region.

It is evident from the tables that line emission becomes important above 25 Å and contributes about 70 percent of the total emission while below 20 Å continuum emission is more important. At higher temperatures, free-free emission dominates over other emissions.

Table 4 shows the principal lines observed below 25 Å with their identification and intensity. Measurements were made by N.R.L. group of workers with high resolution spectrometers.

Table 3

Energy Distribution Between 2 and 20 Å
(E^λ is in erg/cm^2 sec)

	$T = 2 \times 10^6$ °K			
λ(Å)	E_{ff}	E_{fg}	E_L	E^λ
2	1×10^{-16}	1.6×10^{-15}	—	1.70×10^{-15}
3	7.1×10^{-12}	1.14×10^{-10}	—	1.21×10^{-10}
4	1.78×10^{-9}	2.86×10^{-8}	2.25×10^{-11}	3.04×10^{-8}
5	3.16×10^{-8}	5.08×10^{-7}	1.14×10^{-8}	5.51×10^{-7}
6	2.1×10^{-7}	3.37×10^{-6}	2.68×10^{-13}	3.58×10^{-6}
7	1×10^{-6}	1.60×10^{-5}	4.79×10^{-7}	1.75×10^{-5}
8	2.5×10^{-6}	3.99×10^{-5}	3.1×10^{-7}	4.27×10^{-5}
9	5×10^{-6}	7.97×10^{-5}	7.05×10^{-6}	9.17×10^{-5}
10	1×10^{-5}	1.59×10^{-4}	2.88×10^{-6}	1.72×10^{-4}
11	1.26×10^{-5}	1.94×10^{-4}	—	2.07×10^{-4}
12	1.78×10^{-5}	2.74×10^{-4}	2.02×10^{-5}	3.12×10^{-4}
13	2.82×10^{-5}	4.35×10^{-4}	—	4.63×10^{-4}
14	3.55×10^{-5}	5.47×10^{-4}	2.47×10^{-4}	8.29×10^{-4}
15	4.47×10^{-5}	4.43×10^{-4}	1.50×10^{-3}	1.99×10^{-3}
16	5.62×10^{-5}	5.59×10^{-4}	1.08×10^{-3}	1.70×10^{-3}
17	7.1×10^{-5}	7.04×10^{-4}	3.08×10^{-4}	1.08×10^{-3}
18	7.94×10^{-5}	3.23×10^{-4}	4.0×10^{-4}	8.02×10^{-4}
19	8.91×10^{-5}	2.86×10^{-4}	9.28×10^{-3}	9.65×10^{-3}
20	1×10^{-4}	3.02×10^{-4}	8.47×10^{-5}	4.87×10^{-4}

These measurements show a good agreement between experimental observations and theoretical computations. The observed variation of the 20 — 100 Å flux during the solar cycle is in good agreement with theoretical computations. Agreement in the 2 — 20 Å region also becomes good if it is realized that x rays in this wavelength region are emitted primarily by the hot coronal condensation regions. This conclusion has been borne out by x-ray photography of the sun and from the measurements during solar eclipse.

Figure 8 shows the x-ray spectral energy distribution from the quiescent sun from July, 1959, to March, 1964, calculated from the rocket and satellite data. This is a summary of the observed data and shows how variation of flux from solar minima to solar maxima depends upon wavelength.

Conclusion

A substantial volume of experimental and theorietical data on solar x rays is available today, from which it is possible to say:

1. X-ray emission of the quiescent sun is thermal in nature and extends up to a few angstroms in the short-wave end.

2. The 0 — 18 Å spectrum is mainly continuous and is due to recombination emission by the ions of carbon, nitrogen, oxygen, and other elements in the corona. Bremsstrahlung becomes important at higher temperatures.

3. The 18 — 100 Å flux is mainly due to line emission. Continuous bremsstrahlung and recombination emission resulting from the

Table 4

Spectral Energy Distribution Between 20 and 100 Å
(E_λ in erg/cm^2 sec per 5-Å interval)

	Te = 1.10^6 °K					
λ(Å)	E_{ff}	$E_{fg}^{H, He}$	E_{fg}^{heavy}	E_{fg}^{Σ}	E_L	E_λ
100	9.5×10^{-5}	1.97×10^{-4}	—	2.92×10^{-4}	—	2.92×10^{-4}
95	1.97×10^{-4}	4.10×10^{-4}	—	6.05×10^{-4}	1.03×10^{-6}	6.05×10^{-4}
90	2.04×10^{-4}	4.23×10^{-4}	4.70×10^{-5}	6.75×10^{-4}	0.80×10^{-5}	6.83×10^{-4}
85	2.09×10^{-4}	4.35×10^{-4}	4.80×10^{-5}	6.90×10^{-4}	8.3×10^{-4}	1.52×10^{-3}
80	2.14×10^{-4}	4.45×10^{-4}	4.93×10^{-5}	7.05×10^{-4}	0.57×10^{-4}	7.62×10^{-4}
75	2.14×10^{-4}	4.45×10^{-4}	4.93×10^{-5}	7.05×10^{-4}	0.20×10^{-4}	7.25×10^{-4}
70	2.14×10^{-4}	4.45×10^{-4}	4.93×10^{-5}	7.05×10^{-4}	1.83×10^{-4}	8.88×10^{-4}
65	2.09×10^{-4}	4.35×10^{-4}	4.80×10^{-5}	6.90×10^{-4}	5.0×10^{-4}	1.19×10^{-3}
60	2.04×10^{-4}	4.25×10^{-4}	5.30×10^{-5}	6.80×10^{-4}	2.17×10^{-3}	2.85×10^{-3}
55	1.88×10^{-4}	3.91×10^{-4}	4.90×10^{-5}	6.25×10^{-4}	2.79×10^{-3}	3.41×10^{-3}
50	1.81×10^{-4}	3.78×10^{-4}	9.25×10^{-5}	6.50×10^{-4}	3.13×10^{-3}	3.78×10^{-3}
45	1.58×10^{-4}	3.28×10^{-4}	8.05×10^{-5}	5.65×10^{-4}	1.96×10^{-3}	2.52×10^{-3}
40	1.41×10^{-4}	2.93×10^{-4}	9.25×10^{-5}	5.25×10^{-4}	1.44×10^{-2}	1.49×10^{-2}
35	1.1×10^{-4}	2.30×10^{-4}	1.51×10^{-4}	4.91×10^{-4}	3.90×10^{-3}	4.39×10^{-3}
30	7.75×10^{-5}	1.61×10^{-4}	4.36×10^{-4}	6.76×10^{-4}	1.32×10^{-3}	2.0×10^{-3}
25	4.90×10^{-5}	1.02×10^{-4}	7.35×10^{-4}	8.86×10^{-4}	0.18×10^{-4}	9.04×10^{-4}
20	7.05×10^{-6}	1.47×10^{-5}	1.17×10^{-4}	1.39×10^{-4}	2.10×10^{-3}	2.24×10^{-3}
Σ 20-100	2.67×10^{-3}	5.54×10^{-3}	2.09×10^{-3}	1.03×10^{-2}	3.34×10^{-2}	4.37×10^{-2}

Table 5

Relative Contribution of Various Processes to X-Ray Intensity
(flux in erg/cm^2 sec)

Spectral Region	Element (ions)	Type of Emission	Temperature, Te		
			1×10^6 °K	2×10^6 °K	3×10^6 °K
2-10 Å	C, N, O, Mg Si, S, Fe, Ne	Line	5.6×10^{-9}	1.1×10^{-5}	1.40×10^{-4}
		free-free	3.8×10^{-10}	4.1×10^{-7}	6.1×10^{-6}
		free-bound	2.1×10^{-7}	1.95×10^{-4}	1.70×10^{-3}
	H, He	free-free	1.2×10^{-8}	1.3×10^{-5}	2×10^{-4}
		free-bound	1.7×10^{-8}	1.1×10^{-5}	0.96×10^{-4}
		Total Emission:	2.5×10^{-7}	2.4×10^{-4}	2.1×10^{-3}
2-20 Å	C, N, O, Mg Si, S, Fe, Ne	Line	1.2×10^{-4}	1.30×10^{-2}	3.10×10^{-2}
		free-free	2.6×10^{-7}	1.5×10^{-5}	5.3×10^{-5}
		free-bound	1.7×10^{-4}	3.8×10^{-3}	8.2×10^{-3}
	H, He	free-free	8.2×10^{-6}	4.5×10^{-4}	2.0×10^{-3}
		free-bound	1.77×10^{-5}	4.0×10^{-4}	1.0×10^{-3}
		Total Emission:	3.1×10^{-4}	1.80×10^{-2}	4.20×10^{-2}

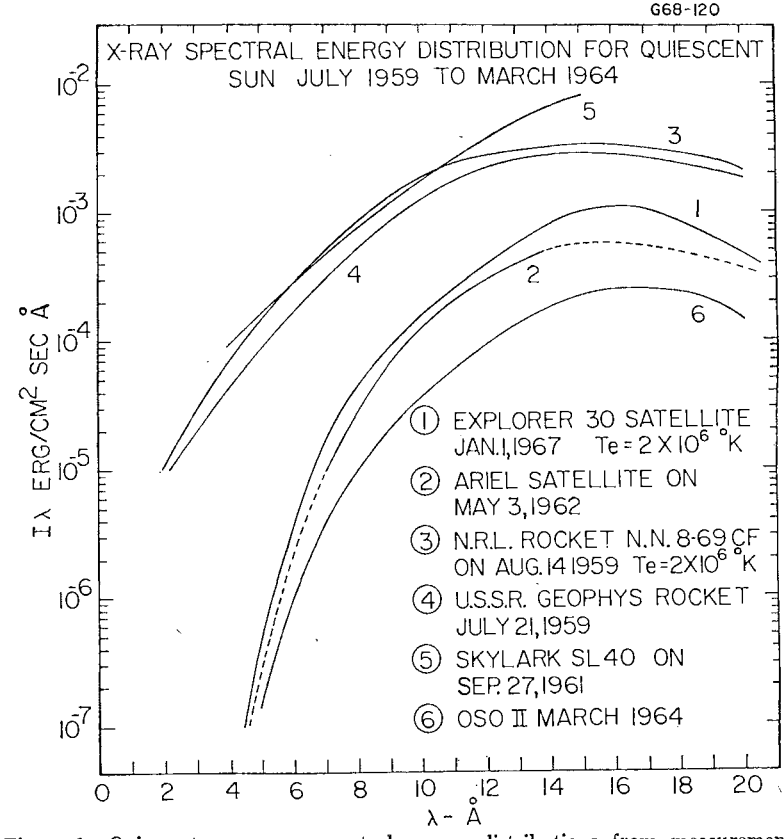

Figure 8. Quiescent sun x-ray spectral energy distributions from measurements made during the period July 1959 to March 1964. (Sunspot maximum to sunspot minimum.)

Table 6

Lines in the Coronal Spectrum Between 13 and 25 Å

Measured Wavelength Å	Lab. or Calculated Wavelength	Intensity Photons/cm^2 sec $\times 10^4$	Ion	Transition	Notes
13.7	13.820	2.1	Fe XVII	2p ^{1}So-3p' ^{1}P$_1$	Possibly also NeIX, narrow
15.0	15.012	16.3	Fe XVII	2p ^{1}So-3d ^{3}P$_1$	narrow
15.25	15.261	10.1	Fe XVII	2p ^{1}So-3d ^{1}P$_1$	narrow
16.0	16.006	5.0	O VII	1s ^{2}S$_{1/2}$-3p ^{2}P$_{3/2,\ 1/2}$	Lβ, narrow
16.72	16.774	15.1	Fe XVII	2p ^{1}So-3s ^{1}P$_1$	narrow
17.01 17.05	17.051	20.1	Fe XVII	2p ^{1}So-3s ^{3}P$_1$	Doubled owing to the deflection of the pointing system, both peaks narrow
17.65 17.72	17.768	22.6	O VII	1s ^{1}So-1s 4p ^{1}P$_1$	Doubled owing to deflection of the pointing system
18.54 18.61	18.627	32.2	O VII	1s^2 ^{1}So-1s 3p ^{1}P$_1$	"
18.8 18.9	18.969	36.0	O VIII	1s S$_{1/2}$-2p ^{2}P$_{3/2,\ 1/2}$	Lα, doubled, wide wings
20.8	20.910	—	N VII	1s^2 ^{1}S$_{1/2}$-3p ^{2}P$_{3/2,\ 1/2}$	Lβ, very weak
21.55	21.602	374.0	O VII	1s^2 ^{1}So-1s 2p ^{1}P$_1$	broad
21.70	21.804	169.0	O VII	1s^2 ^{1}So-1s 2p ^{3}P$_1$	broad
23.2	—	56.5	—	—	broad, not identified, possibly N VI
24.8	24.781	50.9	N VII	1s ^{2}S$_{1/2}$-2p ^{2}P$_{3/2,\ 1/2}$	Lα, broad

interaction of coronal electrons with Hydrogen and Helium ions are important in the continuum emission.

4. X-ray emission, like radio emission, can be divided into a quasi-stable component emitted by undisturbed coronal regions and slowly varying component emitted by active — hotter and denser — coronal regions. Below 20 Å, the contribution due to the quasi-stable component is very small, and the flux is mainly determined by the slowly varying component, i.e., by the coronal condensations. The flux may vary within wide limits, depending on the number, dimensions, density, and temperature of the active regions. The 2 — 8 Å flux varies by a factor of $\approx 10^3$ from solar minima to solar maxima, while the 8 — 20 Å flux varies by a factor of $\approx 10^2$, and the 20 — 100 Å flux varies by a factor of ≈ 10 during the same period.

5. According to x-ray measurements, the temperatures of active coronal regions may reach $2 \times 10^6 - 3 \times 10^6$°K, while the temperature of the undisturbed corona lies between 1.0×10^6 and 1.3×10^6°K. The electron densities in active regions are 5 to 10 times higher than electron densities in the undisturbed regions.

6. Preferred regions of generation of x rays lie above strong calcium plages in the chromosphere and coincide with regions of enhanced centimeter and decimeter radio emission. These regions of increased heating appear to penetrate the entire atmosphere above the photosphere, right up to the corona, and may persist for a considerable time (of the order of a few solar days).

7. Existing theory is capable of predicting the x-ray flux to within a factor of 2 or 3, using solar radio spectro-heliograms in the centimeter range. This opens up important possibilities for short period forecasting of x-ray emission by the quiescent sun.

It may be concluded that the leading features of x-ray emission by the quiescent sun are now adequately understood. Further accumulation of experimental data, particularly in the 0 — 20 Å region with higher spectral resolution, will afford a means for understanding the physics of the solor corona, particularly that of the coronal condensations and active regions. Accurate measurement of x-ray flux in this region with high spectral resolution will also help to test the existing theories of x-ray emission more critically.

ACKNOWLEDGMENT

The author is indebted to Professor J. A. Van Allen for providing the necessary facilities for work and for many useful suggestions.

References

Allen, C. W. 1963. Astrophysical Quantities. 2nd Ed. London: The Athlone Press.

Burnight, T. R. 1949. Phys. Rev., 76, 165.

Chubb, T. A., H. Friedman, R. W. Kreplin, R. L. Blake, and A. E. Unzicker. 1961. Mem. Soc. Roy. Sci. Liege, 4, 228.

Elwert, G. 1954. Zs. Naturforsch., 9a, 637.
Friedman, H. 1962. Reports on Progress in Physics, 25. London: Institute of Physics and the Physical Society.
Friedman, H. 1963. Ann. Rev. Astron. Astrophys., 1, ed. by Leo Goldberg. Palo-Alto: Annual Reviews, Inc.
Kreplin, R. W. 1964. COSPAR Symposium, Florence.
Kreplin, R. W., T. A. Chubb, and H. Friedman. 1962. J. Geophys. Res., 67, 2231.
Sengupta, P. R. 1968. Solar X-Ray Control of the E Layer (to be published).
Sklovskij, I. S. 1949. Izu. Krymsk. astrofiz. obs., 4, 80.
Tousey, R. 1964. Quart., J. Roy. Astron. Soc., 5, 123.
Tousey, R., K. Watanabe, and J. D. Purcell. 1951. Phys. Rev., 83, 792.
Van Allen, J. A. 1967. U. of Iowa Research Report 67-35.